Cell. Mol. Life Sci. (2012) 69:1179–1191
DOI 10.1007/s00018-011-0868-2

Cellular and Molecular Life Sciences

RESEARCH ARTICLE

Homeostatic regulation of NCAM polysialylation is critical for correct synaptic targeting

Johannes Vogt · Robert Glumm · Leslie Schlüter · Dietmar Schmitz · Benjamin R. Rost · Nora Streu · Benjamin Rister · B. Suman Bharathi · Daniel Gagiannis · Herbert Hildebrandt · Birgit Weinhold · Martina Mühlenhoff · Thomas Naumann · Nic E. Savaskan · Anja U. Brauer · Werner Reutter · Bernd Heimrich · Robert Nitsch · Rüdiger Horstkorte

Received: 18 July 2011 / Revised: 5 October 2011 / Accepted: 18 October 2011 / Published online: 9 November 2011

Abstract During development, axonal projections have a remarkable ability to innervate correct dendritic subcompartments of their target neurons and to form regular neuronal circuits. Altered axonal targeting with formation of synapses on inappropriate neurons may result in neurodevelopmental sequelae, leading to psychiatric disorders. Here we show that altering the expression level of the polysialic acid moiety, which is a developmentally regulated, posttranslational modification of the neural cell adhesion molecule NCAM, critically affects correct circuit formation. Using a chemically modified sialic acid precursor (*N*-propyl-D-mannosamine), we inhibited the polysialyltransferase ST8SiaII, the principal enzyme involved in polysialylation during development, at selected developmental time-points. This treatment altered NCAM polysialylation while NCAM expression was not affected. Altered polysialylation resulted in an aberrant mossy fiber projection that formed glutamatergic terminals on pyramidal neurons of the CA1 region in organotypic slice cultures and in vivo. Electrophysiological recordings revealed that the ectopic terminals on CA1 pyramids were functional and displayed characteristics of mossy fiber synapses. Moreover, ultrastructural examination indicated a "mossy fiber synapse"-like morphology. We thus conclude that homeostatic regulation of the amount of synthesized polysialic acid at specific developmental stages is essential for correct synaptic targeting and circuit formation during hippocampal development.

Keywords Hippocampus · Mossy fibers · Synaptic targeting · Glycoengineering · PSA-NCAM · ST8SiaII

B. Heimrich, R. Nitsch, and R. Horstkorte contributed equally as senior authors to this work.

Electronic supplementary material The online version of this article (doi:10.1007/s00018-011-0868-2) contains supplementary material, which is available to authorized users.

J. Vogt (✉) · L. Schlüter · N. Streu · B. Rister · B. Suman Bharathi · R. Nitsch
Institute for Microanatomy and Neurobiology, University Medical Center of the J. Gutenberg, University Mainz, Langenbeckstrasse 1, Bld. 708, 2nd Floor, 55131 Mainz, Germany
e-mail: johannes.vogt@unimedizin-mainz.de

R. Glumm · T. Naumann · A. U. Brauer
Institute for Cell Biology and Neurobiology, Center for Anatomy, Charité–Universitätsmedizin, Berlin, Germany

D. Schmitz · B. R. Rost
Neuroscience Research Center, Charité – Universitätsmedizin Berlin, Berlin, Germany

H. Hildebrandt · B. Weinhold · M. Mühlenhoff
Zelluläre Chemie, Zentrum Biochemie, Medizinische Hochschule Hannover, Hannover, Germany

B. Heimrich
Institute for Anatomy and Cell Biology, Albert Ludwigs, University Freiburg, Freiburg, Germany

W. Reutter
Institute for Biochemistry and Molecular Biology, Charité-Universitätsmedizin, Berlin, Germany

D. Gagiannis · R. Horstkorte
Institut für Physiologische Chemie, Martin-Luther-Universität Halle-Wittenberg, Halle (Saale), Germany

N. E. Savaskan
Department of Neurosurgery, University of Erlangen-Nurnberg, Erlangen, Germany

Introduction

Many molecules that guide axonal pathfinding have been described. However, the mechanisms underlying precise synaptic targeting are largely unknown. Unraveling these mechanisms is thus essential for understanding how neuronal connectivity is accomplished, and for a better understanding of mental diseases that are associated with an altered brain connectivity, such as schizophrenia [1]. Polysialylation is a unique posttranslational modification of the neural cell adhesion molecule (NCAM). Polysialic acid (PSA) expression reaches the highest levels during the formation of neuronal circuits in the perinatal period and, at this stage, largely depends on ST8SiaII, one of two known polysialyltransferases [2]. In the adult brain, PSA expression decreases to basal levels but is upregulated under pathophysiological conditions associated with synaptic plasticity-like temporal lobe epilepsy [3]. This expression pattern indicates that the levels of PSA expression are tightly regulated during development and in the adult brain. However, the role of PSA in the formation of correct neuronal circuits and the effects of altered PSA levels on these circuits remained largely unclear. *ST8SIA2* (SIAT8B, STX) is a candidate susceptibility gene for schizophrenia (for review see [4, 5]) and single-nucleotide polymorphisms in the promoter region of *ST8SIA2* but not of *ST8SIA4* have been linked to schizophrenia [6, 7]. This is in line with findings that single nucleotide polymorphism in the coding region of *ST8SIA2* from schizophrenic patients induced a dramatic decrease of PSA expression [8] and that PSA expression was significantly decreased in the dentate gyrus of schizophrenic patients [9]. All together, these data suggest that homeostatic regulation of PSA expression is critical for correct formation and stability of neuronal circuitry.

A major function of PSA is believed to reside in its anti-adhesive properties controlling NCAM-mediated interaction by masking extracellular parts of the NCAM protein [10–12]. However, neuroanatomical defects that are equally observed in NCAM and PSA-deficient knockout mice suggest a specific function of the PSA proper [10]. This assumption is supported by recent data showing that PSA itself exerts NCAM-independent effects [8, 13–15].

To analyze the effect of PSA on neuronal circuitry formation, we have chosen a new approach using a synthetic sialic acid precursor (*N*-propanoyl-D-mannosamine: ManNProp), which differs in one CH_2 group in the *N*-acyl-side chain from its natural form ManNAc, and acts as a potent inhibitor of the polysialyltransferase ST8SiaII [16–18]. Applying this biochemical inhibition strategy, we have examined the effects of an altered PSA expression on axonal targeting and synaptic specificity at defined developmental time-points in organotypic slice cultures (ex vivo) and in vivo. Hippocampal mossy fiber axons (MF), which express PSA up to adulthood [19], are particularly useful in investigating the role of polysialylation in neuronal circuitry formation for several reasons: (1) they have a layer-specific distribution in the stratum lucidum of the CA3 region, and strictly avoid the CA1 region [20]. This target specificity is a prominent feature of MF and is maintained in organotypic slice cultures [21] and in embryonic transplants in vivo [22]; (2) since PSA-deficient mice have severely damaged axon tracts [10, 12], postnatal alteration of PSA during MF development, allows to study the effect of PSA on MF tract synaptic targeting without bias resulting from mistargeted fiber tracts formed at earlier developmental stages; (3) alterations in the dentate gyrus and in the mossy fibers were described in postmortem brains of patients with schizophrenia and in genetic mouse models for this disease (reviewed in [23]).

Here we show that altering homeostasis of PSA expression via inhibition of ST8SiaII resulted in a loss of target selectivity in vivo with aberrant MF overriding the CA3/CA1 border and entering the CA1 region. Moreover, we found aberrant glutamatergic MF terminals forming inappropriate synapses on CA1 pyramidal cells. Electrophysiological recordings and electron microscopic analysis confirmed that these newly formed MF contacts were in fact functional, glutamatergic, and displayed MF synaptic features such as expression of the presynaptic inhibitory group 2 metabotropic glutamate receptors. These data suggest that PSA synthesis by ST8SiaII at specific developmental time-points has to occur at the right amount and at the right place for correct neuronal connectivity while perturbation of ST8SiaII function may lead to neurodevelopmental deficits similar to those seen in genetic models of schizophrenia.

Materials and methods

Neuraminic acid precursors and measurement of PSA expression

The physiological precursor of neuraminic acid, *N*-acetylmannosamine (ManNAc), was purchased from Sigma. Synthetic derivatives of neuraminic acid precursors with prolonged *N*-acyl-side chains are not commercially available and were synthesized as described [24]. PSA and propyl-PSA (pPSA) expression on cell membranes of slice cultures was measured by Western-blot analysis as described in "Supplemental Material and Methods".

Organotypic slice cultures

Hippocampal slice cultures were prepared from P0 C57BL/6 mice as described previously [25]. For embryonic studies

of the entorhinal perforant path we used slices from E17 C57BL/6 mice. For co-cultures, we positioned the dentate gyrus of wild-type mice either to the CA3 or CA1 region from heterozygous mice that expressed GFP under the ß-actin promoter [26]. In different sets of experiments, slice cultures from the same litter were treated either with 8 mM of the chemically modified sialic acid precursor (ManNProp), 8 mM of the natural sialic acid precursor ManNAc (MP Biomedicals, Solon, OH, USA), or they were left untreated. The glucose concentration of media was adjusted for the additional sialic acid concentration. Tracing of the mossy fiber tract was performed by applying small biocytin crystals onto granule cells of the dentate gyrus. After the cultivation period, slices were fixed with 4% paraformaldehyde (PFA) and processed as described [25].

Immunocytochemistry

Animal experiments and housing were in accordance with the guidelines of European Laboratory Animal Science Associations and were approved by the local ethics committee. Breeding and genotyping of *ST8SiaII*$^{-/-}$ and *ST8SiaII*$^{-/-}$/*ST8SiaIV*$^{-/-}$ mice was performed as described [10]. Treatment of male Sprague–Dawley rats from the same litter was performed after birth every day for 4 weeks with 800 mg/kg s.c. of unnatural sialic acid precursors or with PBS as described [27]. For Timm staining, the brains were cryoprotected, frozen, and sectioned on a cryotome at a thickness of 40 µm. For staining of organotypic slice cultures, slices were fixed in 4% PFA for 2 h and resliced in 50-µm-thick slices. Primary antibodies against NCAM (5B8, 1:1000), PSA (735, 1:1000), propyl-PSA (pPSA) (13D9, 1:1000), calbindin (1:5000, Swant, Bellinzona, Switzerland) and synaptoporin (1:750, Synaptic Systems, Göttingen, Germany) were diluted in blocking solution. For electron microscopy, double stainings were performed using consecutive DAB and DAB Ni/Co as described [28]. Traced mossy fibers were visualized either by conjugation with ABC-Elite complex (Vector Laboratories, Burlingame, CA, USA) followed by DAB visualization or by conjugation with Avidin-Texas Red (Vector Laboratories, Burlingame, CA, USA).

Quantification and statistical analysis

All morphometric measurements were performed on a stereology work station consisting of a modified light microscope, motorized specimen stage, CCD video color camera, and stereology software (StereoInvestigator, Microbrightfield, Williston, VT, USA).

For axonal outgrowth analyses, calbindin-stained mossy fibers from treated and control cultures were imaged with a fluorescent microscope (Olympus, BX 50) equipped with a Cool SNAP ES digital camera (Roper Scientific, Ottobrunn, Germany). Morphometric measurements were performed with the image-analysis software Metamorph (Molecular Devices Corporation, Downington, PA, USA) by investigators blind to experimental conditions. Statistical analyses were calculated with the two-tailed t test. Comparisons between more than two groups were performed by one-way analysis of variance (ANOVA) followed by post hoc Bonferroni tests for pairwise comparisons. Statistical significance was established at $p < 0.05$. All calculations were performed with GraphPad Software (San Diego, CA, USA). Graphs show mean values ± standard error of the mean (SEM). Asterisks indicate statistical significance with $*p < 0.05$, $**p < 0.01$, $***p < 0.001$.

Results

ManNProp treatment decreases PSA expression via ST8SiaII-inhibition

Analysis of NCAM polysialylation in CHO cells revealed that the chemically modified sialic acid precursor ManNProp (formula shown in Fig. 1a) reduced polysialylation by inhibiting ST8SiaII function and not by altering ST8SiaII activity (Fig. 1b) or NCAM biosynthesis (Supplementary Fig. 1). In line, in a more complex environment like the organotypic hippocampal slice cultures, treatment with 8 mM ManNProp reduced the level of PSA expression. However, neurons were able to take up, to metabolize ManNProp and to express chemically modified propyl-PSA (pPSA) thereby preventing the expression of naked NCAM as shown by measuring the level of PSA and pPSA in membranes of slice cultures by Western-blot analysis (Fig. 1c). These results demonstrate a potent inhibition of ST8SiaII-mediated PSA synthesis by ManNProp, resulting in a strong decrease of PSA levels on neuronal membranes during hippocampal development ex vivo.

ST8SiaII inhibition affects fasciculation and targeting of MF

We next investigated the effect of decreased PSA levels on developing neuronal fiber tracts. Hippocampal cultures from newborn mice were treated for 21 DIV (days in vitro) either with 8 mM of the natural precursor ManNAc or with 8 mM ManNProp and compared to untreated cultures. In untreated cultures, hippocampal mossy fibers (MF) fasciculated in the hilus and formed a laminated fiber projection that was confined to the stratum lucidum (SL) of the CA3 region (Fig. 1d). In contrast to ManNAc treatment, after application of ManNProp, the MF projection

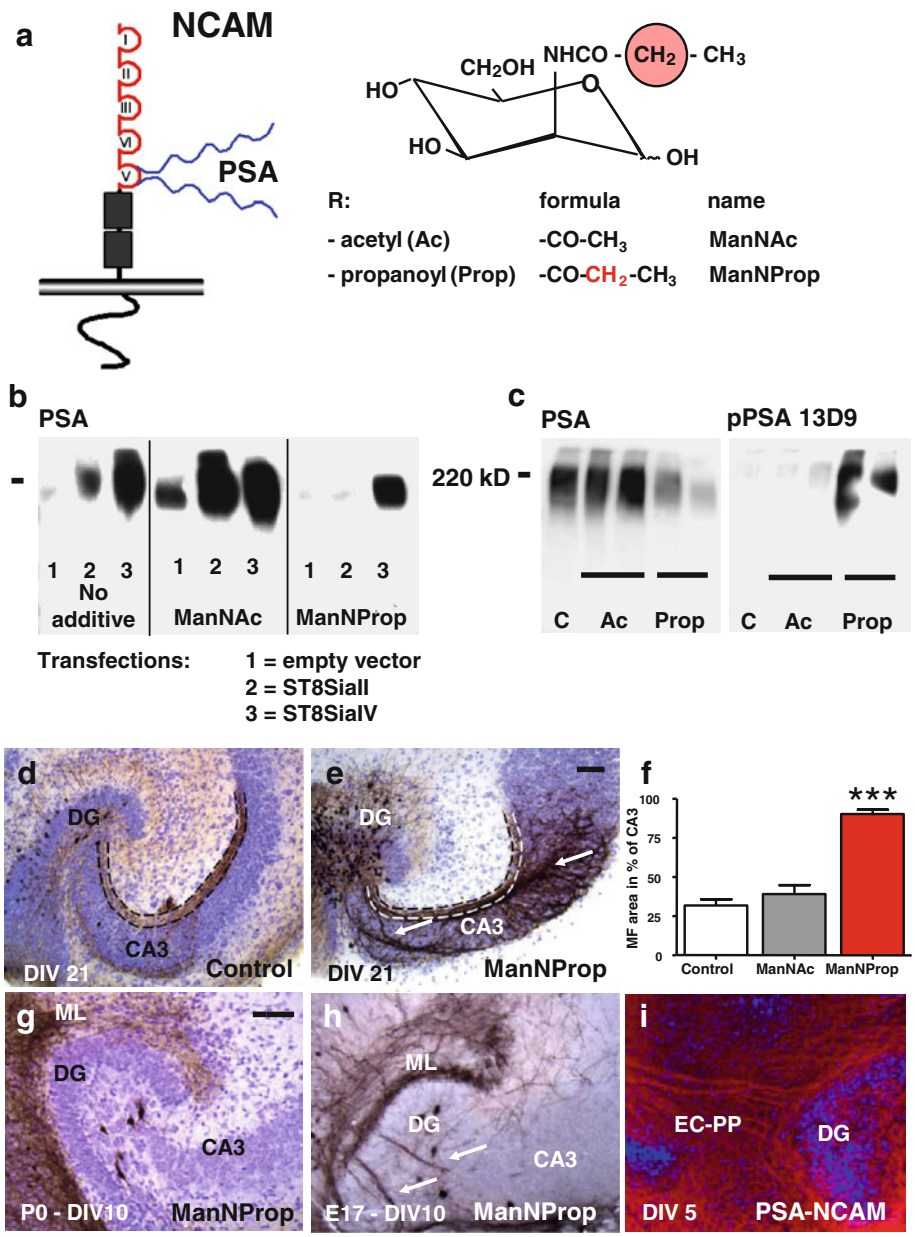

Fig. 1 PSA-depleted axons defasciculate and terminate on aberrant targets. **a** *Left*: schematic illustration of the PSA residue attached to the extracellular portion of NCAM; *Right*: formula of the *N*-acyl-side chain (R) of the naturally occurring sialic acid precursor ManNAc and the chemically modified precursor ManNProp. **b** PSA-negative CHO cells of the complementation group 2A10 expressing PSA-free NCAM were stably transfected with either *ST8SiaII* or *ST8SiaIV* vectors. PSA-NCAM expression on cell membranes was assessed by Western-blot analysis under control conditions and in the presence of 5 mM ManNAc or of 5 mM ManNProp. Normal PSA expression was observed under control conditions and in the presence of ManNAc. In the presence of ManNPorp, only *ST8SiaIV*-transfected cells were capable of polymerizing this unnatural sialic acid derivate and thus expressed polySia, while PSA synthesis in *ST8SiaII*-transfected cells was almost abolished. **c** Western blotting of cell membrane fractions from control organotypic slice cultures (C) and slice cultures treated with ManNAc (Ac) revealed high amounts of PSA (*left*). In contrast, application of ManNProp (Prop) substantially inhibited PSA synthesis on cell membranes. In a similar experiment (*right*), using an antibody specific for ManNProp (13D9), Western-blot analysis showed that ManNPorp was metabolized and expressed on the cell membranes. **d** Suprapyramidal mossy fibers typically converged in the stratum lucidum (marked by *dotted lines*). **e** After inhibiting PSA formation, MF defasciculated (*arrows*) and spread throughout the CA3 pyramidal layer. **f** Area measurements showed a significant aberrant targeting of MF axons after 8 mM ManNProp treatment. **g** The entorhinal perforant path (EC-PP), which started to form prenatally, was not affected by postnatal application of ManNProp. **h** However, when ManNProp application started at an embryonic age (at E17), aberrant perforant path fibers (*arrows*) were observed to pass through the granule cell layer of the DG and to aberrantly target the CA3 pyramidal layer. **i** PSA expression on developing entorhinal fibers (entorhinal perforant path projection, EC-PP). *Scale bar*, 100 µm, $***p < 0.001$

was highly defasciculated, and had left the SL, spreading aberrantly into the entire CA3 pyramidal cell layer (Fig. 1e, arrows). The ratio of aberrant MF invading the CA3 pyramidal region ($n = 9$) was quantified by area measurements that confirmed significant aberrant targeting of MF when compared to controls ($n = 9$) or slice cultures treated with the natural sialic acid precursor ManNAc ($n = 9$) (Fig. 1f). This effect depended on the developmental stage of the axonal projection at the time of altering the PSA synthesis. As shown by the example of the entorhinal perforant path, which starts to form around E17 and expresses PSA-NCAM (Fig. 1i), lowering postnatal PSA expression when first connections were already established, did not affect correct termination (Fig. 1g). In contrast, when inhibition of ST8SiaII started at embryonic stages (E17), these fibers lost their specific termination in the outer molecular layer of the dentate gyrus overriding repulsive properties of the inner molecular layer to aberrantly invade the hilus (Fig. 1h). Our experiments suggest that PSA influences fasciculation and axonal targeting only in a critical developmental time window when the axonal projection starts to grow out.

ManNProp treatment promotes axonal outgrowth

We subsequently investigated the effect of an altered polysialylation on MF outgrowth. At DIV7, the MF projection in slices treated with 8 mM ManNProp had progressed significantly as compared to control slices (Fig. 2a, b). Using identical experimental settings, we measured the fluorescence intensity and the area of calbindin-immunofluorescent MF projections and found a significant axonal outgrowth-promoting effect after ManNProp treatment (Fig. 2c).

Ectopic mossy fibers express NCAM but not PSA-NCAM

Analysis of NCAM expression in organotypic slice cultures revealed that MF expressed NCAM (Fig. 3a, b). After inhibiting ST8SiaII, NCAM-positive MF defasciculated and diffusely distributed into the CA3 pyramidal layer (Fig. 3c). These aberrant fibers expressed calbindin, a marker of mature MF [29] (Fig. 3d). In line, PSA expression clearly coincided with the regular MF pattern in the SL of CA3 (Fig. 3e, f). However, after inhibiting ST8SiaII, PSA immunoreactivity was almost undetectable, being just faintly visible in the stratum lucidum on correctly positioned MF (Fig. 3g, h). Aberrant fibers that had left the stratum lucidum expressed pPSA (Fig. 3 i, j, Supplementary Fig. 3). Of further interest, pPSA was expressed by aberrant MF but was not found in the calbindin-positive en-passant boutons of these aberrant fibers (Fig. 3j, inset). This pattern of pPSA expression by MF but not by MF synapses recapitulated the distribution of PSA immunoreactivity on naive MF [29, 30]. Taken together, these data suggest that PSA-expressing fibers were restricted to their correct termination layer, while loss of PSA after ST8SiaII inhibition allowed axons to cross the borders of their termination area and to form ectopic contacts. However, NCAM expressed at the membranes of aberrant axons was not in a naked form as in *ST8SiaII*$^{-/-}$/*ST8SiaIV*$^{-/-}$ animals, where expression of PSA-negative NCAM impaired axonal outgrowth [12], but was covered by pPSA and therefore did not interfere with the axonal outgrowth capacity as shown in Fig. 2a–c.

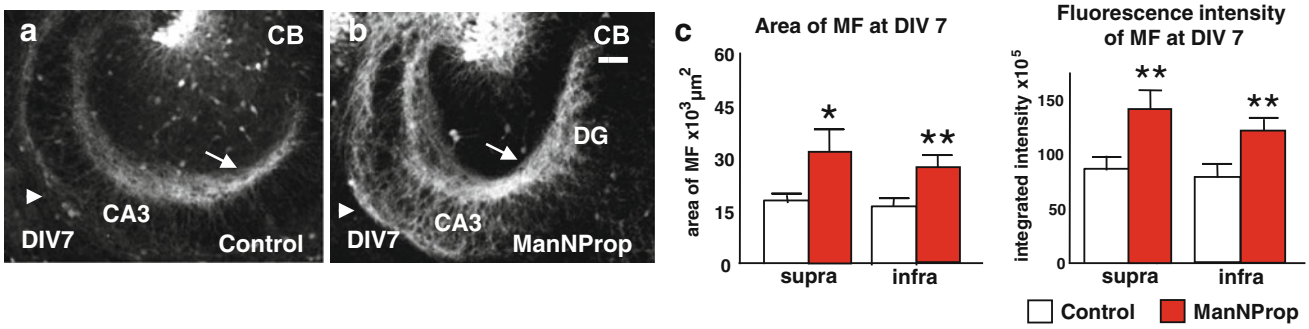

Fig. 2 ManNProp treatment has an axonal outgrowth-promoting effect. **a**, **b** When compared to control slices, inhibition of ST8SiaII by ManNProp had an axonal outgrowth-promoting effect, which was visible on both the suprapyramidal (*arrow*) and infrapyramidal (*arrowhead*) MF bundles. **c** Measurements of the MF area (*left*) and of the integrated signal intensity (*right*) of the calbindin-stained MF axons at DIV 7 confirmed the axonal outgrowth-promoting effect in ManNProp-treated cultures ($n = 12$) compared to control cultures ($n = 15$). This effect was observed for the suprapyramidal portion (supra), as well as for the infrapyramidal portion (infra) of the MF tract. *Scale bar*, 100 µm. *$p < 0.05$, **$p < 0.01$

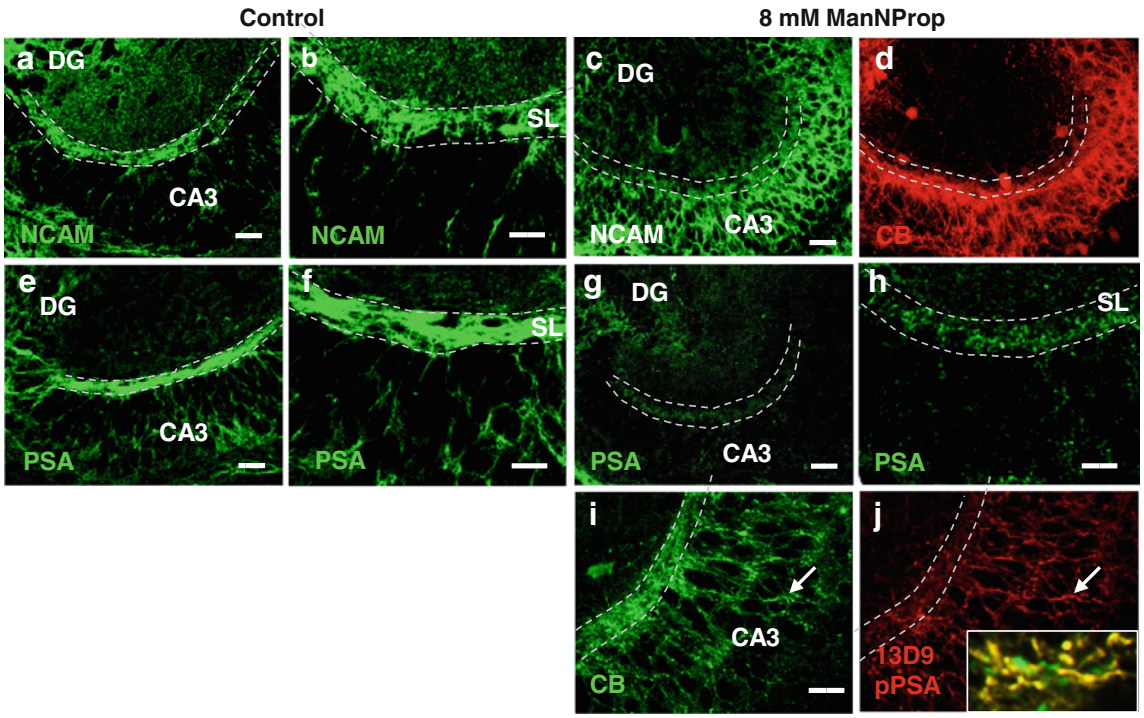

Fig. 3 NCAM and PSA expression in the stratum lucidum of control and ManNProp-treated slices. **a** NCAM is expressed by MF in the stratum lucidum (SL, *dashed line*). **b** Higher magnification shows the strong fasciculation of MF in the SL. **c** After inhibiting the embryonic polysialyltransferase ST8SiaII, PSA-depleted MF lost their lamination and invaded the pyramidal CA3 layer. **d** Staining for calbindin (CB) shows that these aberrant MF have ectopically maturated. **e** MF that run in the SL express PSA. **f** Higher magnification shows the precise lamination of the PSA signal in the SL. **g**, **h** Overview and higher magnification shows that although PSA was markedly decreased, it was still correctly expressed by regularly running MF in the SL (*dashed line*). **i**, **j** Staining for CB and pPSA (derived from metabolized ManNProp) revealed that pPSA was mainly found on aberrant MF (*arrow*). Higher magnification of aberrant pPSA-expressing MF shows co-expression of CB (*inset*). However, pPSA was not found in the CB-positive MF boutons (*inset* and Supplementary Fig. 2). *Scale bars*, 100 μm (**a**, **c**, **e**, **g**), 40 μm (**b**, **d**, **f**, **h**, **i**, **j**)

Electrophysiological coupling of aberrant MF and CA1 neurons

To further investigate as to what extent inhibition of PSA synthesis alters synaptic targeting and connectivity of MF, we co-cultured the dentate gyrus with slices containing either the CA3 or CA1 region. CA1-containing slices from mice expressing GFP under the β-actin promoter [26] were cultivated with non-fluorescent slices to distinguish between the two co-cultured slices (see Supplementary Fig. 4 for schematic representation). While MF were able to enter the CA3 region (Fig. 4c), they were not able to invade this region when confronted with the CA1 region (Fig. 4a). In contrast, ManNProp-treated MF entered the CA1 region for long distances (Fig. 4b, d), even extending into the subiculum in some cultures (data not shown). Stainings for synaptoporin, a marker for presynaptic MF terminals [31], suggested that MF not only entered the CA1 region but also formed presynaptic terminals around CA1 pyramids (Fig. 4e–h).

We have then examined whether these MF contacts on CA1 pyramids represented functional synapses, and performed whole-cell patch clamp recordings from CA1 pyramidal neurons in current-clamp and voltage-clamp mode ($n = 18$, see "Supplemental Material and Methods"). In 15 of 18 such recordings, we found synaptic input from the co-cultured dentate gyrus on CA1 pyramidal neurons (Fig. 4i, upper trace). Other studies have shown that markers of the glutamatergic and GABAergic phenotypes may coexist in developing hippocampal granule cells. Recent electrophysiological data suggest that activation of granule cells produces simultaneous glutamate-receptor-mediated and GABA-receptor-mediated responses in their postsynaptic cells [32]. Such a scenario was unlikely in our experimental conditions since the potent $GABA_A$ receptor antagonist GABAzine did not block the synaptic currents, but induced polysynaptic excitatory postsynaptic currents (EPSC) (see arrow in Fig. 4i, lower left trace) instead. The AMPA/kainate receptor antagonist NBQX completely abolished the synaptic currents (Fig. 4i, lower right trace; 4k). Additionally, MF synapses express presynaptic inhibitory group 2 metabotropic glutamate receptors (mGluRs), whereas associational/commissural synapses do not [33, 34].

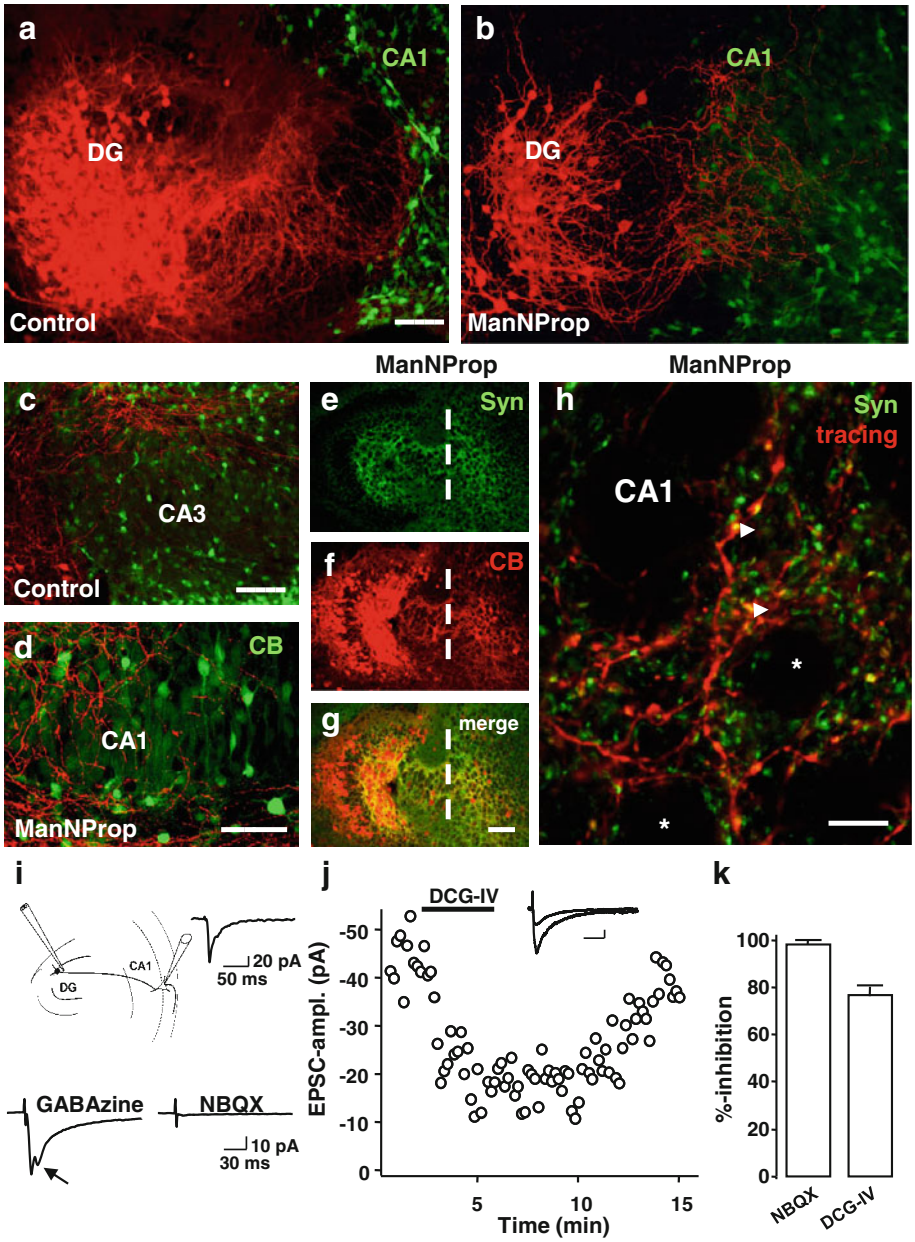

Fig. 4 Altered PSA expression allows MF to form functional synapses on CA1 neurons. **a**, **c** In co-cultures where the DG was cultivated with either CA3 or CA1, biocytin-traced MF show clear region preferences, as they were repelled by CA1 explants (**a**) but were able to innervate the CA3 region (**c**). **b**, **d** After inhibiting PSA synthesis with ManNProp, MF were able to invade the CA1 region (**b**) where they distributed around calbindin-positive CA1 neurons (**d**). **e–g** Calbindin-positive MF invading the CA1 region expressed synaptoporin (Syn). **h** Higher magnification of the CA1 region confirms that traced mossy fibers contacted the CA1 neurons (*) and formed synaptoporin-positive boutons (*arrowheads*). **i** Schematic drawing of the whole-cell patch clamp recording setup. Recordings were taken of CA1 pyramidal neurons while DG granule cells were stimulated. The *upper inset* displays an example of stimulus-evoked postsynaptic currents. *Lower left* trace depicts a similar experiment using the $GABA_A$ receptor antagonist GABAzine. Note the polysynaptic EPSC (*arrow*). As can be seen in the lower right trace, the AMPA/kainate receptor antagonist NBQX completely blocked the EPSCs. **j** The specific mGluR group 2 agonist DCG-IV reversibly inhibited EPSCs. *Scale bars*, 30 ms, 10 pA. **k** A summary of five and six such experiments for NBQX and DCG-IV, respectively. *CB*, calbindin, *Syn*, synaptoporin, *Scale bars*, 100 µm (**a–i**), 25 µm (**j**)

Figure 4j shows an experiment in which the specific mGluR group 2 agonist DCG-IV inhibited dentate gyrus-evoked EPSCs by about 75%, confirming that these contacts on CA1 neurons display MF synaptic features. A summary of six such experiments is shown in Fig. 4k. These experiments substantiate the observation that PSA levels are critical in the synaptic target selectivity of glutamatergic MF terminals and suggest that the excitatory presynaptic MF terminals are sufficient to establish functional and specific synapses on CA1 neurons.

Reduced PSA expression allows MF to form synaptic contacts on CA1 pyramids in vivo

We next assessed the effect of ST8SiaII inhibition on neuronal circuit formation in vivo and treated rats with 800 mg/kg ManNProp as described [27]. The treatment started at postnatal day 1 (P1) and continued for up to 4 weeks after birth, covering the phase when MF grow out and maturate. MF from sham-treated ($n = 5$) (Fig. 5a) and ManNProp-treated littermates ($n = 5$) (Fig. 5b) were visualized by Timm staining. ManNProp-treated rats displayed a significantly longer infrapyramidal MF tract, which is a characteristic phenotype of *ST8SiaII* Ko mice [35], pointing to a specific inhibition of the ST8SiaII by ManNProp (Supplementary Fig. 5a–c). In line with in vivo biochemical studies [27], we observed a lower level of PSA staining on MF in ManNProp-treated mice (Fig. 5g and Supplementary Fig. 5e). However, in addition to the phenotype described in *ST8SiaII* Ko mice, the suprapyramidal MF projection crossed the CA3/CA1 border and entered into the CA1 pyramidal layer, which is characterized by the appearance of small pyramidal cells [20] leading to the typical compact appearance of the Nissl-stained CA1 pyramidal layer (Fig. 5b, c). To confirm that MF have crossed the CA3/CA1 border, we have additionally performed immunostainings, which confirmed that the synaptoporin-positive MF entered the CA1 region that is characterized by the appearance of calbindin-positive pyramids [36]. Interestingly, a similar finding was observed in an animal model for schizophrenia induced by DISC-1 disruption in the presynaptic compartment [37]. Since synaptoporin-positive terminals on CA1 pyramids might also originate from interneurons [31], we have analyzed Timm-stained MF in the CA1 region at higher magnification. Higher magnification (Fig. 5c, inset) revealed abundant Timm-stained MF en-passant boutons around typical CA1 small pyramidal cell bodies supporting MF innervation of CA1 pyramidal neurons. We then analyzed the expression of NCAM and PSA in these aberrant fibers and found a normal NCAM expression (Fig. 5d, e). In contrast, PSA was not expressed on fibers that entered the CA1 region and contacted calbindin-positive CA1 pyramids but was only found on correctly terminating MF fibers in the CA3 region (Fig. 5f, g).

Investigation of the synaptic characteristics of the aberrant MF on the CA1 pyramids showed that these fibers formed synaptoporin and calbindin-positive presynaptic terminals on CB-positive CA1 pyramids (double-labeling in Fig. 5 i, j). To determine whether these aberrant MF synapses on CA1 neurons had an adequate postsynaptic specialization, we performed electron microscopic analysis on identified MF synapses on CA1 neurons (Fig. 5k and inset). Double-immunolabeling against CB (DAB) and synaptoporin (DAB Ni/Co) revealed that the synaptoporin-positive MF terminals contacted the proximal dendritic segment of a presumed calbindin-positive CA1 pyramid (Fig. 5l). Higher magnification shows (Fig. 5l, inset) that this synapse was asymmetric, which is a typical feature of excitatory synapses. However, since the depicted cell could represent a calbindin-positive interneuron—which in the CA3 region is a common target of MF [38], we performed another set of experiments where we combined immunogold (for CB) and DAB (for synaptoporin) detection (Fig. 5m, n). Ultrastructural analysis revealed DAB-stained typical, complex synaptoporin-positive MF terminals forming excitatory contacts with immunogold-stained CB-positive dendrites of CA1 neurons (Fig. 5n). Since we did not observe typical postsynaptic features of MF synapses [39], i.e., large postsynaptic excrescences, we performed Golgi staining of the hippocampus from control and ManNProp-treated animals, which enabled us to investigate the MF typical, postsynaptic, giant thorny excrescences on a large scale [40]. Golgi impregnation of CA1 neurons revealed none of these postsynaptic structural features of MF synapses (Supplementary Fig. 6a–d). These data suggest that PSA expression influences the presynaptic as well as the postsynaptic compartment allowing MF to target ectopic hippocampal subfields where they form new synaptic contacts on inappropriate postsynaptic targets (CA1 instead of CA3).

Retrograde MF innervation and altered spine formation after ST8SiaII inhibition

We next investigated whether the PSA influence on synaptic targeting was restricted to the anterograde MF projection or was a more general phenomenon and analyzed recurrent MF after ManNProp-treatment in vivo. Recurrent MF aberrantly crossed the granule cell layer to terminate on neurons in the molecular layer (Fig. 6b). Such an aberrant innervation was even observed close to the hippocampal fissure (Fig. 6c). This innervation pattern resembled the mossy fiber sprouting observed after kainate induced status epilepticus [41]. Stereological assessment of the recurrent MF confirmed the significant recurrent MF innervation as well as their extension outside the normal termination area (Fig. 6d).

To analyze the influence of native PSA formation via ST8SiaII on the postsynaptic compartment, we treated primary hippocampal neurons with ManNProp for 14 days. Continuous ST8SiaII inhibition resulted in a significant dysregulation of spine development leading to significant spine head shrinkage and spine length reduction (Fig. 6e, f). This finding is in line with the long-term effect observed on spines after DISC-1 disruption [42] and suggests that ST8SiaII-mediated polysialylation during synaptic

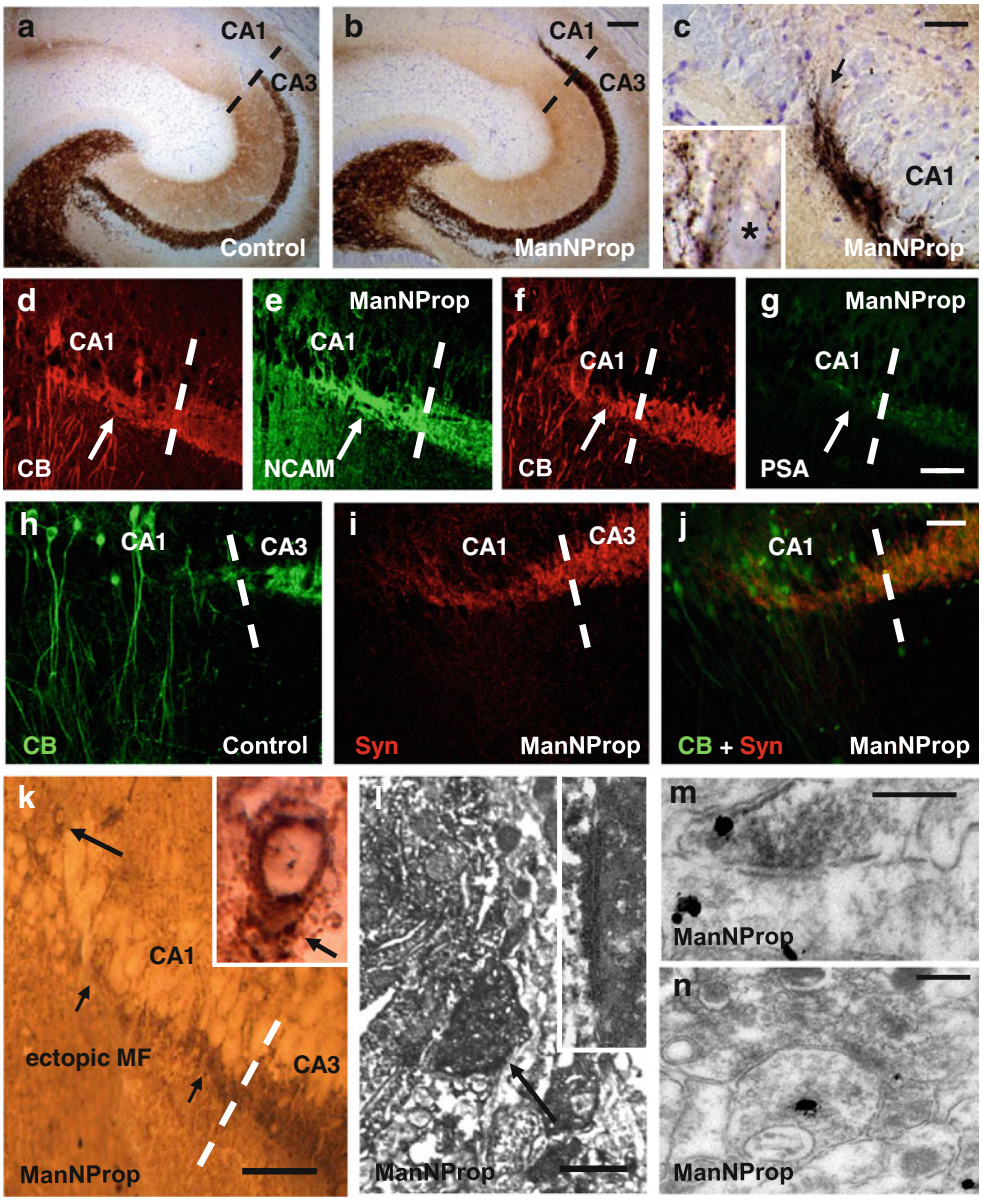

Fig. 5 Altered PSA expression influences MF synaptic targeting in vivo. **a** Timm staining showed a normal MF pattern in the hippocampus of a control rat aged 4 weeks. **b** At the same postnatal age, the suprapyramidal MF tract did not stop at the CA3/CA1 border, but entered the CA1 region. **c** Higher magnification of Timm-stained MF in the CA1 region shows typical presynaptic en-passant boutons in the stratum radiatum (where CA1 dendrites are localized) and around CA1 pyramids (*arrow*). *Inset* shows a CA1 principal cell (*asterisk*) surrounded by MF boutons. **d**, **e** MF in the CA1 region were CB- and NCAM-positive. **f**, **g** In contrast, aberrantly targeting MF did not express PSA. PSA expression was confined to the regularly terminating MF at the CA3 border. **h** In control animals, CB-positive MF stopped at the CA3 border and did not reach the CB-positive CA1 neurons. **i**, **j** MF axons of ManNProp-treated animals crossed the CA3 border forming synaptoporin (Syn)-positive presynaptic terminals around CA1 neurons. **k** Double staining against synaptoporin (dark staining surrounding the neuronal cells in CA1, Ni/Co intensified DAB) and CB (light staining, DAB) showed MF innervation (*small arrows*) of CB-positive CA1 neurons. Higher magnification (*inset*) shows a brown DAB-stained CB-positive presumable CA1 neuron (indicated by the *large arrow* in the overview) contacted by dark DAB-Ni/Co-stained synaptoporin-positive MF terminals. *Arrow* in the *inset* points to the identified terminal, which is shown at ultrastructural level in **l**. **l** Electron microscopy of the identified synaptoporin-positive synaptic contact (*arrow*) on the calbindin-positive neuron shown in the inset in **k** (**l**, *inset*). Higher magnification reveals that the contact was asymmetric, which is a morphological feature of an excitatory synapse. **m** Ultrastructural double-labeling of a DAB-stained synaptoporin-positive MF terminal on an immunogold labeled calbindin-positive CA1 dendrite. Since the MF terminal was also positive for calbindin, immunogold signal could be also observed in this MF terminal. **n** Example of a complex, synaptoporin-positive MF terminal (DAB) in the CA1 region contacting an immunogold labeled calbindin-positive CA1 dendrite. *Scale bar*, 100 μm (**a**, **b**), 50 μm (**c**–**k**), 2 μm (**l**), 200 nm (**m**, **n**)

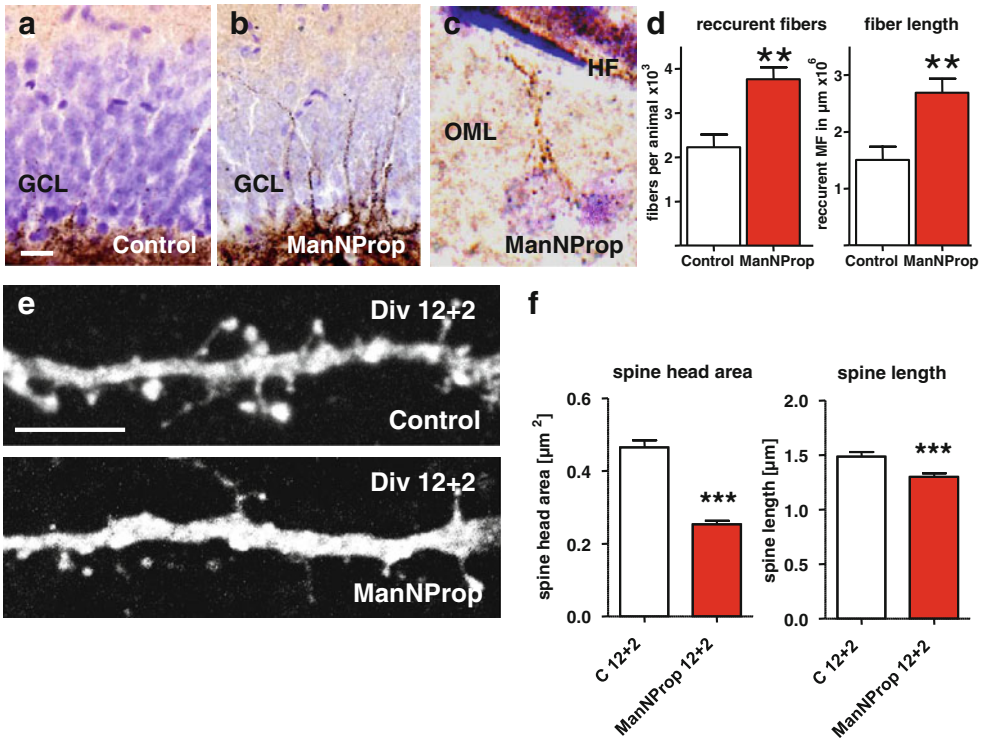

Fig. 6 Retrograde MF innervation and altered spines after ST8SiaII inhibition by ManNProp. **a**, **b** While control animals at 4 weeks show a normal MF innervation pattern as shown by Timm staining (**a**), ManNProp-treated animals display an intense recurrent innervation of the gcl and the molecular layer (**b**). **c** Recurrent innervation was observed even at the border of the outer molecular layer (OML) on a neuron located close to the hippocampal fissure (HF). **d** Stereological assessment of the number and the overall length of the recurrent MF confirms significant recurrent innervation after PSA depletion by ManNProp. **e** When compared to controls, ManNProp-treated neurons displayed smaller spines with a clearly reduced spine head area. **f** Morphometric analysis revealed significantly smaller spines with almost halved spine head areas. *Scale bar* 25 µm (**a**, **b**), 5 µm (**c**, **e**)

formation is important for correct development of the presynaptic as well as of the postsynaptic compartment. Together with previous data and an unaltered NCAM expression, this finding supports the assumption that PSA deficiency itself alters glutamatergic connectivity leading to phenotypes observed under pathophysiologic conditions like epilepsy and schizophrenia.

Effect of constitutive *ST8SiaII* and *ST8SiaII/ST8SiaIV* disruption on MF targeting

Since ManNProp application in vivo represents a targeted biochemical intervention at a specific developmental stage, we analyzed MF formation in constitutive *ST8SiaII*$^{-/-}$ and *ST8SiaII*$^{-/-}$/*ST8SiaIV*$^{-/-}$ mice. Analysis of MF synapses by Timm staining (Fig. 7a, b) and immunostaining of presynaptic MF terminals by calbindin and synaptoporin (Fig. 7 g, h) in *ST8SiaII*$^{-/-}$ mice revealed an attenuated phenotype with some MF beyond the CA3 border contacting calbindin-positive pyramids. However, Timm staining revealed no recurrent MF innervation of the DG (Fig. 7c), suggesting quantitative and qualitative differences in the degree of aberrant MF observed after targeted inhibition of ST8SiaII by ManNProp and constitutive *ST8SiaII* disruption. In line with previous data [10, 12], *ST8SiaII*$^{-/-}$/*ST8SiaIV*$^{-/-}$ mice displayed a rather hypomorphic MF tract, which did not reach the CA1 region nor displayed recurrent MF targeting (Fig. 7d–f, i, j).

Discussion

Polysialylation is a unique, posttranslational modification of NCAM that occurs at embryonic and at early postnatal stages during the formation of neuronal circuitries and, in this time window, mainly relies on the polysialyltransferase ST8SiaII [2]. *ST8SIA2* is a strong candidate gene for schizophrenia predisposition [4, 5], and point mutations in *ST8SIA2* described in schizophrenic patients were found to strongly decrease PSA synthesis [8]. These data are in line with significantly decreased PSA expression in the dentate gyrus of schizophrenic patients [9] and suggest that altered PSA levels during neuronal circuit formation may be the underlying pathology contributing to the development of this disease. Although various knockout animals have been generated [10, 35, 43, 44], the exact functions of PSA are

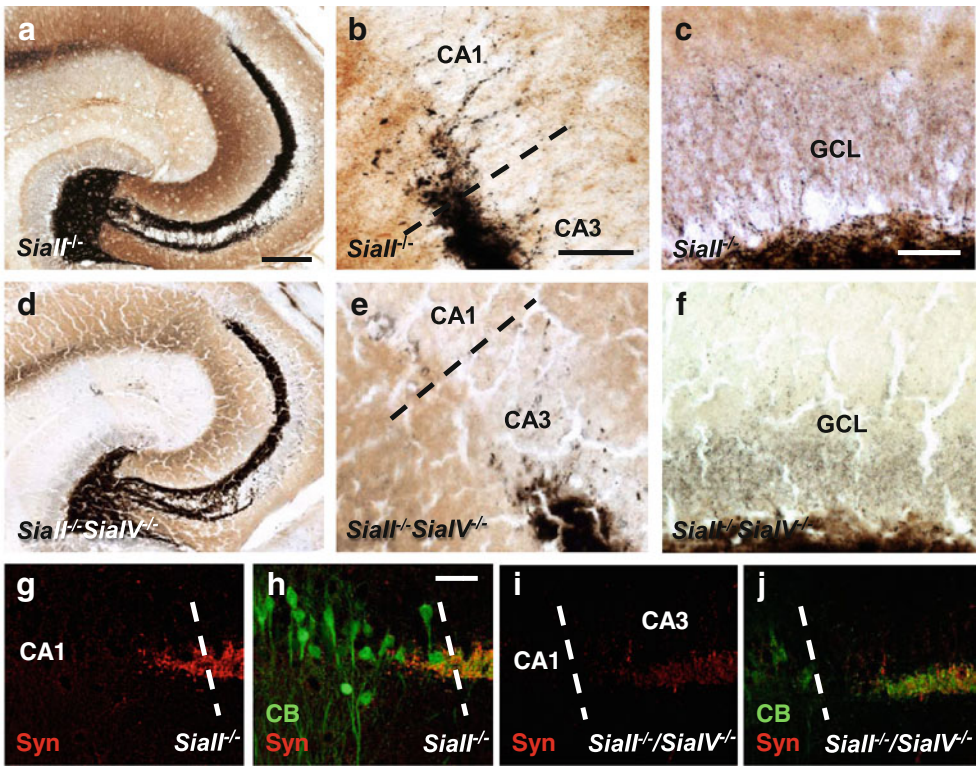

Fig. 7 MF termination in constitutive *ST8SiaII*$^{-/-}$ or *ST8SiaII*$^{-/-}$/*ST8SiaIV*$^{-/-}$ mice (**a–c**). To precisely depict the amount of aberrant MF, Timm staining was depicted without Nissl staining. *ST8Sia2*$^{-/-}$ mice show the typical longer infrapyramidal MF projection [43] while some aberrant MF crossed the CA3 border and entered the CA1 region characterized by the compact morphology resulting from the densely packed small pyramidal CA1 neurons (**b**). However, *ST8Sia2*$^{-/-}$ mice did not display a recurrent innervation of the dentate gyrus (**c**). **d–f** Constitutive *ST8SiaII/ST8SiaIV* deletion does not affect MF targeting at the CA3 border (**e**) or promote a recurrent MF innervation of the molecular layer (**f**). **g**, **h** Aberrant MF crossed the CA3 border, illustrated by the appearance of CB-positive pyramids and innervated these pyramids. **i**, **j** In contrast, MF in *ST8SiaII*$^{-/-}$/*ST8SiaIV*$^{-/-}$ mice did not reach the CA3 border even showing a hypomorphic appearance. *Scale bar* 250 μm (**a**, **d**), 50 μm (**b**, **c**, **e**, **f**, **g–j**)

still debated [45, 46]. Constitutive polysialyltransferase-deficient mice show multiple neurodevelopmental defects ranging from migration deficits, increased apoptotic cell death through to defects in the formation of specific axon tracts [10, 12, 47]. While on the one side the broad range of developmental defects hampers the interpretation of PSA functions, constitutive deficiency prevents investigation of the dynamic regulation of PSA levels during development.

To circumvent the bias derived from developmental deficits, we inhibited ST8SiaII function using *N*-propyl-D-mannosamine (ManNProp), a chemically engineered sialic acid precursor [16–18], at specific developmental time-points. Using this approach, we significantly reduced NCAM polysialylation while minimizing possible compensatory effects (upregulation of ST8SiaIV), which have been described in *ST8SiaII*-deficient animals [10, 48] and which most probably resulted in the unaltered PSA content in the hippocampus described in these animals [35]. A major finding of the present study is that altering PSA levels disrupted axonal and synaptic target specificity of MF, leading to ectopic MF axons that crossed the CA3 border and terminated on CA1 pyramids. Together with enhanced axonal outgrowth, this finding was similar to the MF phenotype described after presynaptic DISC-1 disruption, which is a genetic model for schizophrenia [37].

Analysis of spine formation after ManNProp application showed significant spine shrinkage and correlated with the long-term effect of DISC-1 disruption in spines [42], suggesting that lowering PSA levels and DISC-1 disruption alter targeting of presynaptic terminals as well as the postsynaptic compartment during glutamatergic synapse formation in a similar way. This data is further corroborated by downstream analysis of ManNProp, which revealed downregulation of the 14-3-3ε protein [49], which is encoded by a recently identified susceptibility gene for schizophrenia (YWHAE) [50], and is a downstream target of DISC-1 [51].

In vivo analysis of targeted ST8SiaII inhibition by ManNProp showed that PSA inhibition resulted in aberrant MF axons, which formed ectopic synaptic contacts on calbindin-positive CA1 neurons expressing MF-specific presynaptic proteins like synaptoporin. Interestingly,

ST8SiaII$^{-/-}$ mice displayed an attenuated phenotype supporting the assumption that constitutive ST8SiaII deficiency was counterbalanced by ST8SiaIV as shown by others [48]. Since DISC-1-deficient MF entered the wild-type CA1 region but did not form synaptic contacts on CA1 neurons, MF-CA1 synaptic contacts after ManNProp treatment may be due to PSA inhibition on the postsynaptic compartment, here the CA1 dendrite, which also expresses PSA-NCAM [29, 44]. These data point to a more general function of PSA, suggesting that precise synaptic targeting via PSA-NCAM not only involves targeting of the presynaptic terminals but also prevents postsynaptic targets from inadequate innervations. Electrophysiological analysis showed that the ectopic MF-CA1 synapses were functional and MF-specific while electron microscopic analysis of identified synaptoporin-positive synapses on CA1 calbindin-positive neurons confirmed that these contacts were excitatory. However, these synapses did not display typical postsynaptic features of MF synapses such as large postsynaptic excrescences [39]. These findings reinforce the idea that the CA3 border is not only a repulsive but also a functional barrier for MF.

While NCAM expression on aberrant MF was not affected, which is in line with recent data [48, 52], after inhibiting ST8SiaII by ManNProp, PSA expression was dramatically reduced. PSA, synthesized presumably by ST8SiaIV, was only found at very low levels on correctly extending MF in the stratum lucidum. In line, neurons were able to metabolize ManNProp and to express pPSA on their cell membranes. Interestingly, pPSA was almost exclusively located on aberrant fibers. In contrast to studies that analyzed the effects of PSA loss by EndoN application [19] or in *ST8SiaII*$^{-/-}$/*ST8SiaIV*$^{-/-}$ mice [10, 12], suppression of PSA formation via inhibition of ST8SiaII by ManNProp did not result in a complete loss of PSA and expression of "naked" NCAM. Functional outgrowth experiments suggest that pPSA expression on cell membranes could partially substitute for PSA function counterbalancing gain-of-function effects caused by the expression of PSA-free NCAM [10], which have been described to result in hypoplastic axon tracts [12].

Since (1) detailed analysis revealed an attenuated phenotype of aberrant MF beyond the CA3 border but no retrograde MF sprouting in constitutive *ST8SiaII*$^{-/-}$ mice, and (2) the entorhinal cortex projection was only affected in a critical prenatal period but not by postnatal ST8SiaII inhibition, our data suggest that homeostatic regulation of PSA synthesis leading to the right amount of polysialylated NCAM at the right developmental stage mediates precise targeting of glutamatergic presynaptic terminals while it prevents postsynaptic structures from inadequate innervations. All together, these data show that altered PSA formation via ST8SiaII inhibition lead to profound changes in glutamatergic neuronal connectivity. Together with (1) morphological findings showing a region-specific decrease in PSA expression in the dentate gyrus of patients suffering from schizophrenia [9] and (2) biochemical data showing that SNPs found in schizophrenic patients decreased the amount of PSA [8], our data suggest that affecting homeostasis of NCAM polysialylation may lead to alterations in precise neuronal circuit formation, which in sum may contribute to the development of psychiatric diseases.

Acknowledgments We thank Sabine Nöhring, Katja Rösler, and Dagmar Löck for technical assistance and Richard Hill for critically reading the manuscript. This work was supported by the CRC 971 (J.V. and R.N.) and the DFG He1520 (B.H.); Ho 1959 (R.H.). N.E.S. is supported by the International Human Frontier Science Program Organization (HFSP).

Conflict of interest The authors declare that they have no conflicts of interest.

References

1. Lewis DA, Levitt P (2002) Schizophrenia as a disorder of neurodevelopment. Annu Rev Neurosci 25:409–432
2. Hildebrandt H, Muhlenhoff M, Gerardy-Schahn R (2010) Polysialylation of NCAM. Adv Exp Med Biol 663:95–109
3. Mikkonen M et al (1998) Remodeling of neuronal circuitries in human temporal lobe epilepsy: increased expression of highly polysialylated neural cell adhesion molecule in the hippocampus and the entorhinal cortex. Ann Neurol 44(6):923–934
4. Vawter MP (2000) Dysregulation of the neural cell adhesion molecule and neuropsychiatric disorders. Eur J Pharmacol 405(1–3):385–395
5. Brennaman LH, Maness PF (2010) NCAM in neuropsychiatric and neurodegenerative disorders. Adv Exp Med Biol 663:299–317
6. Arai M et al (2006) Association between polymorphisms in the promoter region of the sialyltransferase 8B (SIAT8B) gene and schizophrenia. Biol Psychiatry 59(7):652–659
7. Tao R et al (2007) Positive association between SIAT8B and schizophrenia in the Chinese Han population. Schizophr Res 90(1–3):108–114
8. Isomura R, Kitajima K, Sato C (2011) Structural and functional impairments of polysialic acid by a mutated polysialyltransferase found in schizophrenia. J Biol Chem 286(24):21535–21545
9. Barbeau D et al (1995) Decreased expression of the embryonic form of the neural cell adhesion molecule in schizophrenic brains. Proc Natl Acad Sci USA 92(7):2785–2789
10. Weinhold B et al (2005) Genetic ablation of polysialic acid causes severe neurodevelopmental defects rescued by deletion of the neural cell adhesion molecule. J Biol Chem 280(52):42971–42977
11. Rockle I et al (2008) Polysialic acid controls NCAM-induced differentiation of neuronal precursors into calretinin-positive olfactory bulb interneurons. Dev Neurobiol 68(9):1170–1184
12. Hildebrandt H et al (2009) Imbalance of neural cell adhesion molecule and polysialyltransferase alleles causes defective brain connectivity. Brain 132:2831–2838

13. Kochlamazashvili G et al (2010) Neural cell adhesion molecule-associated polysialic acid regulates synaptic plasticity and learning by restraining the signaling through GluN2B-containing NMDA receptors. J Neurosci 30(11):4171–4183
14. Kanato Y, Kitajima K, Sato C (2008) Direct binding of polysialic acid to a brain-derived neurotrophic factor depends on the degree of polymerization. Glycobiology 18(12):1044–1053
15. Storms SD, Rutishauser U (1998) A role for polysialic acid in neural cell adhesion molecule heterophilic binding to proteoglycans. J Biol Chem 273(42):27124–27129
16. Mahal LK et al (2001) A small-molecule modulator of poly-alpha 2, 8-sialic acid expression on cultured neurons and tumor cells. Science 294(5541):380–381
17. Charter NW et al (2002) Differential effects of unnatural sialic acids on the polysialylation of the neural cell adhesion molecule and neuronal behavior. J Biol Chem 277(11):9255–9261
18. Horstkorte R et al (2004) Selective inhibition of polysialyltransferase *ST8SiaII* by unnatural sialic acids. Exp Cell Res 298(1):268–274
19. Seki T, Rutishauser U (1998) Removal of polysialic acid-neural cell adhesion molecule induces aberrant mossy fiber innervation and ectopic synaptogenesis in the hippocampus. J Neurosci 18(10):3757–3766
20. Lorente de No R (1934) Studies on the structure of the cerebral cortex II. Continuation of the study of the ammonic system. J Psychol Neurol 46:113–177
21. Zimmer J, Gahwiler BH (1987) Growth of hippocampal mossy fibers: a lesion and coculture study of organotypic slice cultures. J Comp Neurol 264(1):1–13
22. Fonseca M et al (1992) Monoclonal antibodies to late-differentiating epitopes identify mossy fibre terminals innervating normal and transplanted hippocampal CA3 pyramidal cells. Eur J Neurosci 4(5):448–458
23. Kobayashi K (2009) Targeting the hippocampal mossy fiber synapse for the treatment of psychiatric disorders. Mol Neurobiol 39(1):24–36
24. Keppler OT et al (1995) Biosynthetic modulation of sialic acid-dependent virus-receptor interactions of two primate polyoma viruses. J Biol Chem 270(3):1308–1314
25. Brinks H et al (2004) The repulsive guidance molecule RGMa is involved in the formation of afferent connections in the dentate gyrus. J Neurosci 24(15):3862–3869
26. Okabe M et al (1997) 'Green mice' as a source of ubiquitous green cells. FEBS Lett 407(3):313–319
27. Gagiannis D et al (2007) Engineering the sialic acid in organs of mice using N-propanoylmannosamine. Biochim Biophys Acta 1770(2):297–306
28. Hollerbach EH et al (1998) Region-specific activation of microglial cells in the rat septal complex following fimbria-fornix transection. J Comp Neurol 390(4):481–496
29. Schuster T et al (2001) Immunoelectron microscopic localization of the neural recognition molecules L1, NCAM, and its isoform NCAM180, the NCAM-associated polysialic acid, beta1 integrin and the extracellular matrix molecule tenascin-R in synapses of the adult rat hippocampus. J Neurobiol 49(2):142–158
30. Seki T, Arai Y (1999) Different polysialic acid-neural cell adhesion molecule expression patterns in distinct types of mossy fiber boutons in the adult hippocampus. J Comp Neurol 410(1):115–125
31. Singec I et al (2002) Synaptic vesicle protein synaptoporin is differently expressed by subpopulations of mouse hippocampal neurons. J Comp Neurol 452(2):139–153
32. Gutierrez R (2005) The dual glutamatergic-GABAergic phenotype of hippocampal granule cells. Trends Neurosci 28(6):297–303
33. Kamiya H, Shinozaki H, Yamamoto C (1996) Activation of metabotropic glutamate receptor type 2/3 suppresses transmission at rat hippocampal mossy fibre synapses. J Physiol 493(Pt 2):447–455
34. Nicoll RA, Schmitz D (2005) Synaptic plasticity at hippocampal mossy fibre synapses. Nat Rev Neurosci 6(11):863–876
35. Angata K et al (2004) Sialyltransferase *ST8Sia-II* assembles a subset of polysialic acid that directs hippocampal axonal targeting and promotes fear behavior. J Biol Chem 279(31):32603–32613
36. Sloviter RS (1989) Calcium-binding protein (calbindin-D28 k) and parvalbumin immunocytochemistry: localization in the rat hippocampus with specific reference to the selective vulnerability of hippocampal neurons to seizure activity. J Comp Neurol 280(2):183–196
37. Faulkner RL et al (2008) Development of hippocampal mossy fiber synaptic outputs by new neurons in the adult brain. Proc Natl Acad Sci USA 105(37):14157–14162
38. Acsady L et al (1998) GABAergic cells are the major postsynaptic targets of mossy fibers in the rat hippocampus. J Neurosci 18(9):3386–3403
39. Blackstad TW, Kjaerheim A (1961) Special axo-dendritic synapses in the hippocampal cortex: electron and light microscopic studies on the layer of mossy fibers. J Comp Neurol 117:133–159
40. Represa A, Ben-Ari Y (1992) Kindling is associated with the formation of novel mossy fibre synapses in the CA3 region. Exp Brain Res 92(1):69–78
41. Sloviter RS et al (2006) Kainic acid-induced recurrent mossy fiber innervation of dentate gyrus inhibitory interneurons: possible anatomical substrate of granule cell hyper-inhibition in chronically epileptic rats. J Comp Neurol 494(6):944–960
42. Hayashi-Takagi A et al (2010) Disrupted-in-Schizophrenia 1 (DISC1) regulates spines of the glutamate synapse via Rac1. Nat Neurosci 13(3):327–332
43. Cremer H et al (1998) Long-term but not short-term plasticity at mossy fiber synapses is impaired in neural cell adhesion molecule-deficient mice. Proc Natl Acad Sci USA 95(22):13242–13247
44. Eckhardt M et al (2000) Mice deficient in the polysialyltransferase *ST8SiaIV*/PST-1 allow discrimination of the roles of neural cell adhesion molecule protein and polysialic acid in neural development and synaptic plasticity. J Neurosci 20(14):5234–5244
45. Südhoff TC (2003) The synaptic cleft and synaptic cell adhesion. In: Südhof TC, Cowan WM, Stevens CF (eds) Synapses. The Johns Hopkins University Press, Baltimore
46. Dalva MB, McClelland AC, Kayser MS (2007) Cell adhesion molecules: signalling functions at the synapse. Nat Rev Neurosci 8(3):206–220
47. Angata K et al (2007) Polysialic acid-directed migration and differentiation of neural precursors are essential for mouse brain development. Mol Cell Biol 27(19):6659–6668
48. Galuska SP et al (2006) Polysialic acid profiles of mice expressing variant allelic combinations of the polysialyltransferases *ST8SiaII* and *ST8SiaIV*. J Biol Chem 281(42):31605–31615
49. Buttner B et al (2002) Biochemical engineering of cell surface sialic acids stimulates axonal growth. J Neurosci 22(20):8869–8875
50. Ikeda M et al (2008) Identification of YWHAE, a gene encoding 14–3-3epsilon, as a possible susceptibility gene for schizophrenia. Hum Mol Genet 17(20):3212–3222
51. Taya S et al (2007) DISC1 regulates the transport of the NUDEL/LIS1/14–3-3epsilon complex through kinesin-1. J Neurosci 27(1):15–26
52. Oltmann-Norden I et al (2008) Impact of the polysialyltransferases *ST8SiaII* and *ST8SiaIV* on polysialic acid synthesis during postnatal mouse brain development. J Biol Chem 283(3):1463–1471